Ionization Kinetics of the Carbon Acid Phenindione

V. J. STELLA ˣ **and R. GISH**

Received December 14, 1978, from the *Department of Pharmaceutical Chemistry, University of Kansas, Lawrence, KS 66045.* Accepted for publication February 20, 1979.

Abstract □ The ionization kinetics of carbon acids are slow relative to those of classical acids and bases. Phenindione (2-phenyl-1,3-indandione) is a 1,3-diketone carbon acid of macroscopic experimental pKa 4.09 at 25° and ionic strength 0.1. The ionization kinetics of phenindione were determined at an ionic strength of 0.1 and 25° using stopped-flow spectrophotometry and a pH jump technique. A log k'_{obs}–pH profile for the approach to the ionization equilibrium was determined, and a mechanism consistent with the profile was postulated. The percent enol *versus* diketo form of phenindione and the pKa_{enol} and pKa_{diketo} were calculated from the kinetic data. Phenindione acid deprotonation kinetics by various oxygen and nitrogen bases suggested that, with bases of pKa 4.7–8.5 and in the pH 5–8.5 range, the acidic phenindione proton was ~45% transferred in the rate-determining transition state.

Keyphrases □ Phenindione—ionization kinetics, stopped-flow spectrophotometric and pH analysis, model □ Anticoagulants—phenindione, ionization kinetics, pH □ Kinetics, ionization—phenindione

Phenindione (I) (2-phenyl-1,3-indandione) is an anticoagulant used in patients where the more popular anticoagulants are contraindicated. It is a 1,3-diketone carbon acid [lit. pKa 4.13 (1), 4.10 (2), 5.4 (3)]. Recent work (4, 5) suggested that some of the nonclassical phase transport behavior of another carbon acid, phenylbutazone, might be accounted for by its relatively slow ionization rate. Noninstantaneous ionization is a characteristic of some carbon acids (6–10).

The ionization kinetics of phenindione have not been studied previously, although the ionization kinetics of other carbon acids of much higher pKa's than those of phenindione and phenylbutazone have been well documented in the chemical literature (6–24). The immediate objective of this study was to determine the kinetics and mechanism of ionization of phenindione and to compare its behavior to that of phenylbutazone. Studying the kinetics and mechanism of ionization of a number of carbon acids of varying acidity might permit accurate prediction of the ionization kinetics of other pharmaceutically significant carbon acids. The ultimate objective is to use this information, combined with current ongoing mass transport studies, to predict the effect of noninstantaneous ionization kinetics on the mass transport behavior of carbon acids.

EXPERIMENTAL

Materials—Phenindione[1] was used as received. All reactions and pKa determinations were carried out in double-deionized, carbon dioxide-free water, freshly deoxygenated with oxygen-free nitrogen. The sodium chloride used to adjust the ionic strength was analytical reagent quality and was used without further purification. Hydrochloric acid, acetic acid–acetate, phosphate, and imidazole buffers were prepared with analytical grade components without further purification.

Pyridine, 3-methylpyridine (3-picoline), and morpholine were freshly purified by fractional distillation from potassium hydroxide pellets and stored over molecular sieves. A buffer component, 4-methoxypyridine, was prepared by the catalytic reduction of 4-methoxypyridine-*N*-oxide[2] using a literature method (25) for the reduction of 4-ethoxypyridine-*N*-oxide to 4-ethoxypyridine.

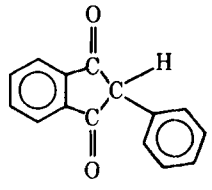

I

pKa Determination—The pKa of phenindione was determined spectrophotometrically[3] (26) at 326 nm and the same temperature and ionic strength conditions as in the kinetic studies, *i.e.*, 25 ± 0.2° and μ = 0.1 (sodium chloride). The pKa's of the various buffers used in the kinetic studies were determined potentiometrically using a pH meter[4] standardized with a standard buffer to a pH near the expected buffer component pKa (26).

Kinetic Studies—The procedures used to follow phenindione ionization kinetics were similar to those previously described for phenylbutazone (4). The reactions were followed at 326 nm, and the initial phenindione concentration was 1×10^{-4} *M*. At a pH where the primary reaction was the protonation of the mesomeric phenindione anion to phenindione acid, phenindione at pH ~7 was jumped to acidic pH (hydrochloric acid buffer or acetate buffer). At a pH where the primary reaction was the phenindione acid deprotonation to the mesomeric anion, phenindione in an aqueous solution of μ = 0.1 and with pH adjusted to ~4 with hydrochloric acid was jumped to the final pH by mixing with a buffer of desired final pH but double the desired final concentration.

The pH values after solution mixing were determined independently by mixing equal volumes of the phenindione solution and the buffer component. In most cases, the final pH was identical to that of the buffer solution. The exceptions were the most dilute morpholine buffer concentrations (see *Results and Discussion*), the hydrochloride acid buffer (final hydrochloric acid concentration was half the initial concentration), and one study where an unbuffered phenindione solution (pH ~4) was mixed with a very dilute sodium hydroxide solution (2×10^{-4} *M*). In this last case, the final pH was 8.91, even though the pH was expected to be closer to 10. The pH's used to construct the pH profile (Fig. 1) for the hydrochloric acid solutions and the sodium hydroxide solution were those measured experimentally.

RESULTS AND DISCUSSION

Figure 2 shows the phenindione UV spectrum under basic as well as acidic conditions, 0.1 *M* NaOH and 0.1 *M* HCl, respectively. The strong bathochromic shift from acidic to basic pH conditions is due to the extended conjugation on ionization, *i.e.*, coupling of the two phenindione phenyl rings through the enolate double bond (1). The macroscopic dissociation constant of phenindione was determined by observing the change in absorbance of a 1×10^{-4} *M* phenindione solution (25° and μ = 0.1) at pH 1 (0.1 *M* HCl), in the pH 2–6 range (acetate buffer), and at pH 13 (0.1 *M* NaOH).

The K_a was determined from a plot of $(A - A_0)[H^+]$ *versus* A as described previously (4), where A is the phenindione absorbance at a given hydrogen-ion concentration, $[H^+]$, and A_0 is the phenindione absorbance under acid conditions, *i.e.*, with the ionization completely suppressed (0.1 *M* HCl). The K_a under the experimental conditions was 8.13×10^{-5}, giving a pKa of 4.09. This value compares favorably with the literature pKa values (1–3) when differences in ionic strength and solvent composition are considered.

Table I gives the observed rate constants, k_{obs} (sec^{-1}), for phenindione ionization kinetics under various pH and buffer concentrations. All observed rate constants are the mean of three or more determinations. Also

[1] Pfaltz and Bauer, Flushing, N.Y.
[2] Aldrich Chemical Co., Milwaukee, Wis.
[3] Cary 15, Cary Instruments, Monrovia, Calif.
[4] Model 701, Orion Research, Cambridge, Mass.

0022-3549/79/0800-1042$01.00/0

Table I—Effect of pH and Buffers on the Ionization Kinetics of Phenindione at 25 ± 0.2° and μ = 0.1 with Sodium Chloride

pH[a]	Buffer (pKa; Concentration Range; Number of Concentrations Studied)	k'_{obs}, sec^{-1}	k_{CAT}, M^{-1} sec^{-1}
1.62	Hydrochloric acid (NA[b]; 0.024 *M*; NA)	262	NA
1.65	Hydrochloric acid (NA; 0.022 *M*; NA	258	NA
2.04	Hydrochloric acid (NA; 0.009 *M*; NA)	198	NA
2.05	Hydrochloric acid (NA; 0.009 *M*; NA)	206	NA
2.05	Hydrochloric acid (NA; 0.009 *M*; NA)	190	NA
2.58	Hydrochloric acid (NA; 0.0026 *M*; NA)	112	NA
2.66	Hydrochloric acid (NA; 0.0025 *M*; NA)	97	NA
2.94	Hydrochloric acid (NA; 0.00115 *M*; NA)	63	NA
3.06	Hydrochloric acid (NA; 0.00087 *M*; NA)	54	NA
3.09	Hydrochloric acid (NA; 0.00081 *M*; NA)	50	NA
3.45	Hydrochloric acid (NA; 0.00035 *M*; NA)	28	NA
5.00	Acetate (4.70; 0–0.05 *M*; 4)	6.3	938 ± 48
6.00	Acetate (4.70; 0–0.05 *M*; 4)	6.0	845 ± 18
6.50	3-Methylpyridine (5.75; 0–0.05 *M*; 4)	7.1	4475 ± 128
7.00	3-Methylpyridine (5.75; 0.03 *M*; 3)	6.8	4900 ± 56
5.00	Pyridine (5.28; 0–0.05 *M*; 3)	8.1	803 ± 10
6.00	Pyridine (5.28; 0–0.05 *M*; 4)	6.9	2489 ± 54
6.20	4-Methoxypyridine (6.64; 0–0.04 *M*; 4)	6.9	1797 ± 58
6.80	4-Methoxypyridine (6.64; 0–0.04 *M*; 4)	7.0	3694 ± 127
7.00	Imidazole (7.10; 0–0.05 *M*; 3)	9.1	2407 ± 94
7.50	Imidazole (7.10; 0–0.025 *M*; 5)	4.7	4310 ± 131
7.00	Morpholine (8.53; 0–0.035 *M*; 3)	7.5	122 ± 61
7.50	Morpholine (8.53; 0–0.035 *M*; 3)	6.0	3660 ± 1
8.00	Morpholine (8.53; 0–0.01 *M*; 5)	13.2	12150 ± 240
8.50	Morpholine (8.53; 0–0.008 *M*; 4)	26	26500 ± 288
7.00	Phosphate (6.75; 0–0.0165 *M*; 3)	5.0	2271 ± 216
7.50	Phosphate (6.75; 0–0.0165 *M*; 3)	7.9	2615 ± 26
8.91	Sodium hydroxide (NA; 1 × 10^{-4} *M*; NA)	61	NA

[a] Experimentally measured final pH. [b] NA = not applicable.

included in this table are the observed rate constants extrapolated to zero buffer concentrations, k'_{obs} (sec^{-1}), obtained from plots of k_{obs} *versus* total buffer concentration. Figure 1 is a plot of log k_{obs} *versus* pH from the phenindione ionization.

A possible model for phenindione ionization kinetics is given in Scheme I, where K is the diketo form of phenindione and the predominant neutral form of phenindione in aqueous solution (1), E is the enol form of phenindione, and E^- is the so-called mesomeric anion (7). The macroscopic dissociation constant for phenindione is defined by:

$$K_a = \frac{[E^-][H^+]}{[K] + [E]} \qquad \text{(Eq. 1)}$$

which can be rearranged to:

$$\frac{1}{K_a} = \frac{1}{K_{a,diketo}} + \frac{1}{K_{a,enol}} \qquad \text{(Eq. 2)}$$

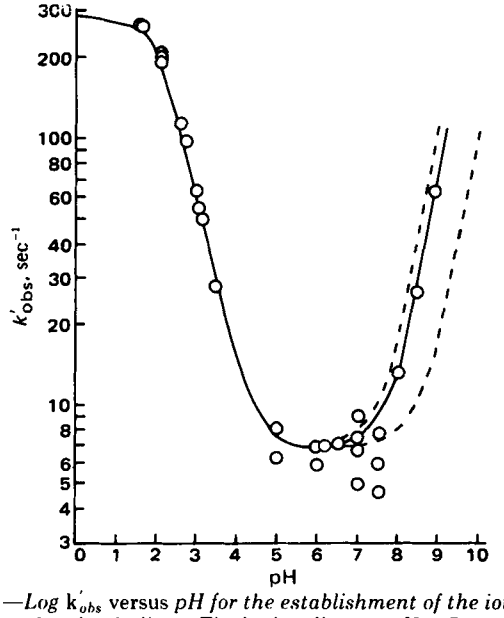

Figure 1—*Log* k'_{obs} versus *pH for the establishment of the ionization equilibrium for phenindione. The broken lines at pH > 7 represent* k_3 *having the limits of* 10^6–10^7 M^{-1} sec^{-1}. *The lack of reproducibility of the data at pH > 8 precludes placing an accurate value on* k_3.

Equation 2 shows the relationship between the macroscopic dissociation constant, K_a, and the microscopic constants, $K_{a,diketo}$ and $K_{a,enol}$. The percent enol present in aqueous solution will be defined by the relative values of $K_{a,diketo}$ and $K_{a,enol}$. The percent enol is defined by:

$$\% \text{ enol} = \frac{[E]}{[K] + [E]} (100) \qquad \text{(Eq. 3)}$$

which can be rearranged to:

$$\% \text{ enol} = \frac{K_{a,diketo}}{K_{a,diketo} + K_{a,enol}} \left(\frac{100}{1}\right) \qquad \text{(Eq. 4)}$$

The assumption can be made that the equilibrium defined by $K_{a,enol}$ is rapid and instantaneous[5] (7). The rate constant k_1 represents the water-catalyzed phenindione deprotonation, k_3 is the hydroxide-ion-catalyzed deprotonation rate constant, and k_{GB} is the general base-catalyzed deprotonation rate constant. The constant k_2 represents the hydronium-catalyzed protonation constant, *i.e.*, the addition of a proton at C-2 of the mesomeric anion; k_4 is the water or spontaneous protonation rate constant, and k_{GA} is the general acid-catalyzed protonation rate constant.

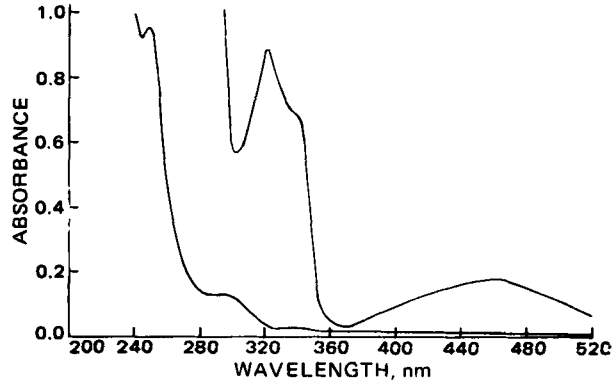

Figure 2—*Phenindione (1 × 10⁻⁴ M) UV spectrum in 0.1 M NaOH (upper curve) and in 0.1 M HCl (lower curve).*

[5] The word instantaneous is used to describe phenomena taking place at rates near the diffusion-controlled limit.

Table II—Final pH after Mixing Equal Volumes of the Initial Morpholine Buffer Solution (Double the Final Concentration) with the Phenindione Solution [a]

Initial Buffer pH	Buffer Concentration (after Mixing), M	Measured Final pH
8.00	2×10^{-3}	7.80[b]
8.00	4×10^{-3}	7.94
8.00	6×10^{-3}	7.98
8.00	8×10^{-3}	8.00
8.00	10×10^{-3}	8.00
8.50	2×10^{-3}	8.44[b]
8.50	4×10^{-3}	8.49
8.50	6×10^{-3}	8.50
8.50	8×10^{-3}	8.50
8.50	10×10^{-3}	8.50

[a] Aqueous phenindione solution of $\mu = 0.1$ with sodium chloride and added hydrochloric acid sufficient to give a pH of ~4. [b] As expected, both of these buffers gave negative deviations in plots of k_{obs} *versus* $[buffer]_T$ so neither was used in the k_{CAT} calculations.

With the assumption of Scheme I, an equation for the approach to the ionization equilibrium can be derived for any perturbation of that equilibrium (4):

$$k'_{obs} = k_1 + k_3[OH^-] + \frac{k_2[H^+]K_{a,enol}}{K_{a,enol} + [H^+]} + \frac{k_4 K_{a,enol}}{K_{a,enol} + [H^+]} \quad \text{(Eq. 5)}$$

For example, if a pH ~ 7 phenindione solution is perturbed rapidly (in the stopped-flow apparatus) to pH ~ 2, the first reaction is the instantaneous protonation of the mesomeric anion to the enol, E, and eventually (at equilibrium) to a mixture of the enol and diketo phenindione forms. Similarly, an acidic phenindione solution perturbed to alkaline pH involves primarily the deprotonation of the diketo phenindione and the small fraction of enol to the mesomeric anion. The observed buffer independent rate constant for the attainment of equilibrium, k'_{obs}, is the sum of both the forward and reverse rate constants because the system under study is a reversible reaction.

UV spectroscopic studies (1) showed that phenindione exists predominantly in its diketo form in aqueous solution. This means (Eq. 4) that $pKa_{diketo} \gg pKa_{enol}$ so that $pKa_{diketo} \sim pKa$ and $pKa_{enol} \ll 4.09$. From Fig. 1, phenindione deprotonation to form the anion, *i.e.*, pH > pKa_{diketo}, the k'_{obs} can be given by:

$$k'_{obs} = k_1 + \frac{k_4 K_{a,enol}}{K_{a,enol} + [H^+]} + k_3[OH^-] \quad \text{(Eq. 6)}$$

and since $K_{a,enol} \gg [H^+]$ at the pH's in question, Eq. 6 simplifies to:

$$k'_{obs} = (k_1 + k_4) + k_3[OH^-] \quad \text{(Eq. 7)}$$

As discussed previously (4), k_4 is negligible relative to k_1, so the plateau seen in Fig. 1 in the pH 5–7.5 range is essentially due to k_1. The constant k_1 calculated as the mean values of k'_{obs} in the pH 6.0–7.0 range was 6.9 sec^{-1}.

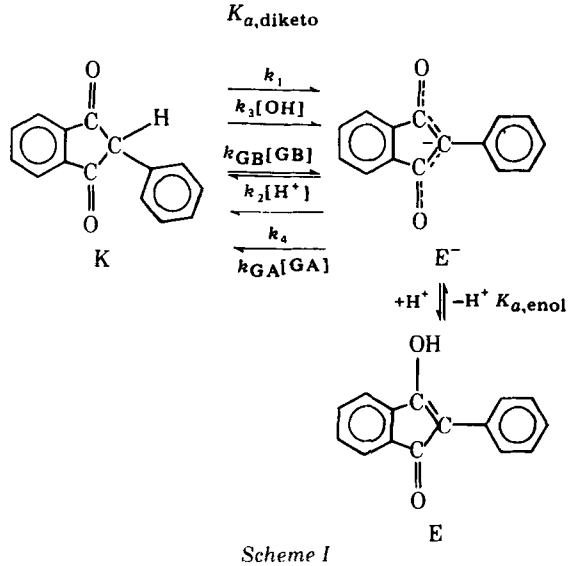

Scheme I

Table III—Kinetic and Equilibrium Constants for Phenindione Ionization at 25° and $\mu = 0.1$ with Sodium Chloride

Parameter	Value
k_1	$6.9\ sec^{-1}$
k_2	$6.5 \times 10^4\ M^{-1}\ sec^{-1}$
k_3	$\sim 6 \times 10^6\ M^{-1}\ sec^{-1}$
k_4	$\sim 5.5 \times 10^{-4}\ sec^{-1}$
$K_{a,enol}$	4.24×10^{-3} ($pKa_{enol} = 2.37$)
$K_{a,diketo}$	1.06×10^{-4} (pKa = 3.97)
K_a	1.03×10^{-4} (pKa = 3.99[a])
	8.13×10^{-5} (pKa = 4.09[b])
% enol	2.4

[a] Determined kinetically. [b] Determined spectrophotometrically.

The limited number of points and the questionable accuracy of the unbuffered hydroxide-ion solution reaction given on the last line of Table I allow only a crude k_3 estimate of between 10^6 and $10^7\ M^{-1}\ sec^{-1}$. For the sake of fitting the observed data to Eq. 5, $6 \times 10^6\ M^{-1}\ sec^{-1}$ was used for k_3. In an earlier study with phenylbutazone (4), borate buffers, which are poor proton-abstracting agents, were used at pH 8.5–9.5. Recent papers and some earlier work suggested that the ionization kinetics of borate buffers themselves are slow (27–33). This then raises the question as to what was the microscopic pH upon perturbing an acid solution of the carbon acid to an alkaline pH maintained with a borate buffer.

In the present study, when a borate buffer study was undertaken in the pH 8.5–9.5 range, an estimate of k_3 of closer to $1 \times 10^6\ M^{-1}\ sec^{-1}$ was made. This would suggest that the earlier k_3 estimate for phenylbutazone deprotonation by hydroxide ion may be low. Unfortunately, other techniques for following fast reactions cannot be applied to the deprotonation reactions in question. Even though k_{obs} is in the measurable range (by stopped-flow spectrophotometry) at pH 8–9, the pH after mixing must be maintained with a buffer of sufficient buffer capacity. Normally, the buffer concentration is varied and plots of k_{obs} *versus* buffer concentrations are extrapolated to zero buffer concentration to obtain k'_{obs}. This approach was attempted with morpholine buffer at pH 8.00 and 8.50 (Table I) and concentrations after mixing of below $1 \times 10^{-2}\ M$.

Table II gives the final pH values after the morpholine buffers were mixed with the phenindione solution (pH ~ 4 with hydrochloric acid). At the low buffer concentrations, significant pH alterations, affecting both the hydroxide-ion concentration and the fraction of total morpholine present in the the unionized state, occurred. Higher buffer concentrations or stronger bases could not be used because the deprotonation reaction became too rapid to be followed by stopped-flow spectrophotometry. The phenindione solution had to be somewhat acidic so that sufficient spectral alteration would occur as a result of the pH perturbation to allow the reaction to be followed spectrophotometrically.

At pH < 8, the $k_3[OH^-]$ term is negligible and, since k_4 is small relative to all other terms:

$$k'_{obs} = k_1 + \frac{k_2[H^+]K_{a,enol}}{K_{a,enol} + [H^+]} \quad \text{(Eq. 8)}$$

which can be rearranged to:

$$\frac{1}{k'_{obs} - k_1} = \frac{1}{k_2[H^+]} + \frac{1}{k_2 K_{a,enol}} \quad \text{(Eq. 9)}$$

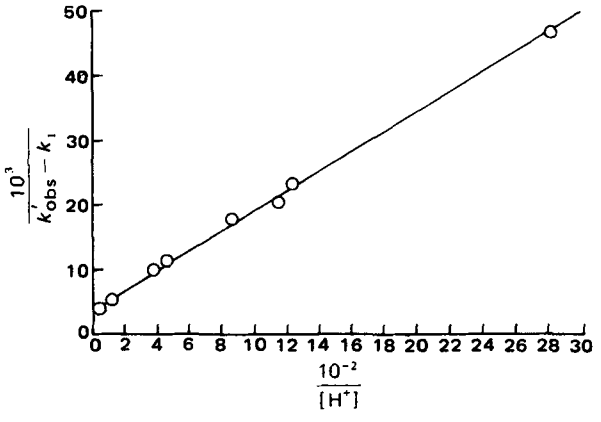

Figure 3—*Plot used to determine* k_2 *and* $K_{a,enol}$ *for phenindione ionization (Eq. 9 and Scheme I).*

predicting that a plot of the left side of Eq. 9 against $1/[H^+]$ should give a straight line of slope $1/k_2$ and intercept $1/k_2K_{a,enol}$, thus allowing both k_2 and $K_{a,enol}$ to be calculated. Such a plot for phenindione is shown in Fig. 3. The calculated values of k_2 and $K_{a,enol}$ are $6.5 \times 10^4\ M^{-1}\ sec^{-1}$ and $4.24 \times 10^{-3}\ M$, respectively ($pK_{a_{enol}} = 2.37$).

According to Scheme I, the equilibrium ionization constant for diketo phenindione is:

$$K_{a,diketo} = \frac{k_1}{k_2} = \frac{6.9}{6.5 \times 10^4} = 1.06 \times 10^{-4}\ M \qquad \text{(Eq. 10)}$$

Having determined $K_{a,enol}$ and $K_{a,diketo}$ and using Eq. 4, the enol was calculated at 2.4%.

Table III summarizes the kinetic and equilibrium constants calculated. The values for rate constants from Table III were placed into Eq. 5 to generate a theoretical curve for phenindione ionization kinetics at various pH's, assuming the mechanism shown in Scheme I. The solid line drawn in Fig. 1 is the line generated by Eq. 5 and the appropriate values in Table III. Apparently, Eq. 5 and Scheme I adequately describe the observed values, although other mechanisms may be possible (4).

A comparison of the values of k_1 and k_2, the two most accurately determined rate constants for both phenylbutazone and phenindione, highlights some interesting points. The lower pKa of phenindione relative to phenylbutazone, 3.99 *versus* 4.33, is due to changes in both k_1 and k_2. *A priori*, based on the strength of the acids, k_1 for phenindione (the stronger acid) would be expected to be greater than that for phenylbutazone. Such is not the case. The constant k_1 has a value of 6.9 sec^{-1} for phenindione compared to 10.1 sec^{-1} for phenylbutazone. The small differences in k_1, ~30%, are more than compensated by the differences in k_2. The constant k_2 has a value of $6.5 \times 10^4\ M^{-1}\ sec^{-1}$ for phenindione relative to $2.1 \times 10^5\ M^{-1}\ sec^{-1}$ for phenylbutazone. The greater acidity of phenindione relative to phenylbutazone is controlled not by how readily the acid gives up its proton but by the ability of its base form to accept a proton.

Equation 5 appears to describe adequately phenindione protonation and deprotonation kinetics in the absence of buffer species capable of acting as general acids and bases. In the presence of acids and bases other than the water species, the observed rate constant for the approach to the ionization equilibrium after a pH perturbation would be given by:

$$k_{obs} = k'_{obs} + k_{GB}[GB] + \frac{k_{GA}[GA]K_{a,enol}}{[H^+] + K_{a,enol}} \qquad \text{(Eq. 11)}$$

and since at pH > 4, $K_{a,enol} \gg [H^+]$, Eq. 11 reduces to:

$$k_{obs} = k'_{obs} + k_{GB}[GB] + k_{GA}[GA] \qquad \text{(Eq. 12)}$$

$$k_{obs} = k'_{obs} + k_{CAT}\,[buffer]_T \qquad \text{(Eq. 13)}$$

where k_{CAT} is the observed catalytic rate constant for any buffer at any given pH value. This is equal to:

$$k_{CAT} = k_{GB}f + k_{GA}(1 - f) \qquad \text{(Eq. 14)}$$

$$k_{CAT} = f(k_{GB} - k_{GA}) + k_{GA} \qquad \text{(Eq. 15)}$$

where f is equal to the fraction of total buffer species in the base form and $(1 - f)$ is the fraction of total buffer species in its acid form at any given pH. For any given singly dissociating buffer species with a known dissociation constant, f can be calculated from:

$$f = \frac{[H^+]}{K'_a + [H^+]} \qquad \text{(Eq. 16)}$$

where K'_a is the dissociation constant of the conjugate acid form of the buffer. Equation 13 predicts that a plot of k_{obs} *versus* total buffer concentrations, $[buffer]_T$, would be linear with slope k_{CAT} and intercept k'_{obs}. A plot of k_{CAT} *versus* f is predicted from Eq. 15 to be linear with an intercept at $f = 0$ of k_{GA} and an intercept at $f = 1$ of k_{GB}. With the buffers studied, acetate, phosphate, pyridine, 3-methylpyridine, 4-methoxypyridine, imidazole, and morpholine, all plots of k_{obs} *versus* total buffer concentration were linear. From plots of k_{CAT} *versus* f, for all cases except acetic acid, k_{GA} was negligible relative to k_{GB}. When a small or even slightly negative intercept at $f = 0$ was seen from plots of k_{CAT} *versus* f, k_{GB} was calculated from k_{CAT}/f and the mean values of k_{GB} for the various bases calculated at different pH's are recorded in Table IV. Table IV is a compilation of the calculated k_{GA} and k_{GB} values for all of the buffers and water species.

A Brønsted plot (19, 23, 34) of log k_{GB} *versus* the pKa''s of the various buffers is given in Fig. 4. When studying a limited number of bases (acetate through morpholine in the present study) for a reaction catalyzed by general bases, apparent linear Brønsted plots usually result (19, 23).

Table IV—Calculated k_{GA} and k_{GB}

Buffer (pKa)	k_2, k_4, or k_{GA}, $M^{-1}\ sec^{-1}$	k_1, k_3, or k_{GB}, $M^{-1}\ sec^{-1}$
H_3O^+ (−1.74)	6.5×10^4	—
H_2O (−1.74 and 15.74)[a]	1×10^{-5} (5.5 $\times 10^{-4}$/55.5)[b]	1.24×10^{-1} (6.9/55.5)[b]
Acetic acid (4.70)	1161	828
Pyridine (5.28)	263	3635
3-Methylpyridine (5.75)	—[c]	5210[c]
4-Methoxypyridine (6.64)	—[c]	6458[c]
Imidazole (7.10)	—[c]	5728[c]
Morpholine (8.53)	—[c]	48123[c]
Phosphoric acid (2.12)	1223[d]	1223[d]
Phosphoric acid (6.75)	—	2861[d]
OH^- (15.74)	—	6×10^6

[a] When H_2O is acting as a base, its conjugate acid is H_3O^+. When H_2O is acting as an acid, its conjugate base is OH^-. [b] From the kinetic study, it was possible to calculate the rate constants for H_2O acting both as an acid and a base. [c] Plots of k_{CAT} *versus* gave either negligible k_{GA} values or slightly negative values. Therefore, k_{GB} was calculated as the mean value for k_{CAT}/f for each pH studied. [d] This refers to $H_2PO_4^-$ acting as either a general acid or a general base. Because of this ambiguity, the point for $H_2PO_4^-$ was not included in Fig. 4. It is not possible to determine in what capacity $H_2PO_4^-$ is acting. Although HPO_4^{2-} is capable of acting either as an acid or a base, it is more likely acting as a base.

It is becoming increasingly obvious that over a more extensive range of bases, nonlinear Brønsted plots, especially for the ionization kinetics of carbon acids, are more the rule than the exception (6, 7, 19, 23). The reason behind the nonlinearity was first discussed by Eigen (7) and quantitated recently by the Marcus theory (23, 35).

The Marcus theory of general base catalysis suggests that a quadratic fit to the Brønsted plot is more accurate and reflects more closely the mechanism of such catalysis. The solid curved line drawn through the points in Fig. 4 is the quadratic fit[6] to the data. The number of bases studied in the present work was limited by the speed of the reaction. Of course, the catalytic effect of water acting as a base could be determined because of its high intrinsic concentration (55.5 *M*), and hydroxide-ion catalysis could be approximately determined because its effective concentration could be determined from pH measurements.

The solid curved line in Fig. 4 is described by:

$$\log k_{GB} = -1.36 \times 10^{-2}\,pKa'^2 + 6.25 \times 10^{-1}\,pKa' + 2.76 \times 10^{-1} \qquad \text{(Eq. 17)}$$

Differentiation of Eq. 17 would give the slope of the line at any point and is described by Eq. 18. For a Brønsted plot, the slope for general base-catalyzed reactions is given the designation β:

$$\beta = \frac{d(\log k_{GB})}{d(pKa')} = -2.72 \times 10^{-2}\,pKa' + 0.625 \qquad \text{(Eq. 18)}$$

The Brønsted plot resulting from the present study could just as easily be described by a linear plot, with the H_2O term and the OH^- term giving

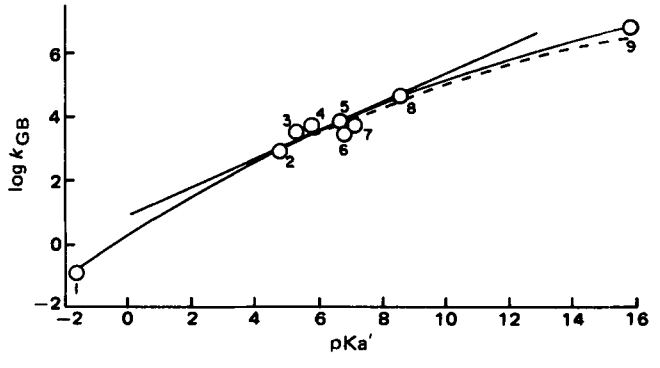

Figure 4—*Log* k_{GB} versus *pKa' for phenindione deprotonation by various general bases of varying pKa. Key: 1, water; 2, acetate; 3, pyridine; 4, 3-methylpyridine; 5, 4-methoxypyridine; 6, monohydrogen phosphate; 7, imidazole; 8, morpholine; and 9, hydroxide ion.*

[6] Least-squares analysis; TI59 programmable calculator utilizing the solid-state statistic module.

negative deviations from the linear plot. Such a plot would be given by the solid straight line in Fig. 4. The slope of the line is 0.45.

The Marcus theory states that when the pKa′ of the general base is equal to the carbon acid pKa, β, the slope of the Brønsted plot, should be equal to 0.5. Substitution of 3.99 for the phenindione pKa into Eq. 18 gives a β value of 0.52. Kresge (23) and Hupe and Wu (19) recently attempted to interpret the nonlinear Brønsted plots often seen for the ionization of various carbon acids. The Marcus theory (35) for such curvature relates the free energy of activation, $\Delta G^{\neq}$, for the proton transfer process to the energy required to bring the reactants together, Wr, and the intrinsic energy involved in the proton transfer, $(1 + \Delta G_0/4\Delta G_0^{\neq})^2\Delta G_0^{\neq}$, as defined by Eq. 19. The term ΔG_0 is the free energy for proton transfer at equilibrium, and $\Delta G_0^{\neq}$ is the free energy of activation for the proton transfer when $\Delta G_0 = 0$. That is, ΔG_0 is equal to zero when the pKa′ of the general base is equal to the pKa of the carbon acid:

$$\Delta G^{\neq} = (1 + \Delta G_0/4\Delta G_0^{\neq})^2\Delta G_0^{\neq} + Wr \qquad \text{(Eq. 19)}$$

The term ΔG_0 can be calculated from:

$$\Delta G_0 = -RT \ln(K_a'/K_a) \qquad \text{(Eq. 20)}$$

From the quadratic fit to the general base data (Eq. 17), k_{GB} at pKa′ 3.99 was calculated to be 357 M^{-1} sec^{-1}; $\Delta G^{\neq}$, calculated by solving for $\Delta G^{\neq}$ from:

$$k_{GB} = 10^{12.74} e^{-\Delta G^{\neq}/RT} \qquad \text{(Eq. 21)}$$

is equal to 13,899 cal/mole (~13,900 cal/mole). It is possible to relate the first coefficient (pKa′^{2} term) of Eq. 17, a, directly to the term $\Delta G_0^{\neq}$ through (23):

$$a = \frac{2.303RT}{16\Delta G_0^{\neq}} \qquad \text{(Eq. 22)}$$

thus allowing $\Delta G_0^{\neq}$ to be calculated. A value of ~6300 cal/mole was thus determined for $\Delta G_0^{\neq}$. Having calculated $\Delta G_0^{\neq}$ as ~6300 cal/mole and $\Delta G^{\neq}$ as ~13,900 cal/mole, at pKa′ = pKa, Wr can be estimated as ~7600 cal/mole. By using the values for $\Delta G_0^{\neq}$ of 6300 cal/mole and Wr of 7600 cal/mole, $\Delta G^{\neq}$ from the full range of bases (H_2O–OH^-) can be calculated and compared to the quadratic fit to Eq. 17. The broken line in Fig. 4 is the line generated from Eqs. 19 and 21. Note that the broken line was generated from Eqs. 19 and 21 using the information that, at pKa′ 3.99, the two lines should have intersected. That is, the solid curved line and the curved broken line intersect at pKa′ 3.99.

The interpretation of these observations is that carbon acid deprotonation involves two processes: (*a*) a work term, which includes desolvation of the incoming base and alteration in the solvation around the reaction center as well as getting the molecule in the correct configuration for proton abstraction, and (*b*) the energy required for breaking the carbon–hydrogen bond. The Wr term in Eq. 19, which is considered to be the work required to bring the two reacting molecules together, has an energy requirement of 7600 cal/mole, which is a little more than the energy required to break a hydrogen bond (36). Similarly, the standard free energy of activation, $\Delta G_0^{\neq}$, which is related to the intrinsic barrier to the breaking of the carbon–hydrogen bond, also has an energy requirement that is a little more than that required to break a weak carbon hydrogen bond (36).

In the past, the apparent negative deviation of hydroxide ion in linear Brønsted plots was always interpreted as the "anomolous" behavior of hydroxide ion. A study involving proton abstraction from a weak carbon acid (19) recently showed that hydroxide-ion behavior is not "anomalous" when other weak oxygen acids are included; *i.e.*, hydroxide ion acted as predicted for a base of pKa 15.74. The Brønsted plot curvature was interpreted as a change in the rate-determining step in going from weak bases to strong bases such as hydroxide ions. That is, with weak bases, the major rate-determining factor is the carbon–hydrogen bond breaking (first term in Eq. 19 is dominant) while with stronger bases the work term, Wr, begins to dominate. The reverse of this step (protonation of the mesomeric anion by a water molecule) has shown similarly anomalous kinetic behavior, suggesting that solvent reorganization around the reaction center may contribute to the rate-determining step (4, 37). As discussed previously (19), the alternative mechanism of a gradual change only in the degree of proton transfer in going from weak to stronger bases does *not* appear to be reasonable for the nonlinear Brønsted plot, although this mechanism cannot be totally ruled out.

If the Brønsted slope, β, *does* approximate the degree of a proton transfer over a limited pKa′ range for weak bases (23), it can be seen from Fig. 4 that a Brønsted slope of 0.45 is calculated for bases with a pKa′ of 4.7–8.53. An interpretation of this result is that the phenindione proton is 45% transferred in the rate-determining transition state for proton abstraction by these bases. A way of testing the hypothesis that a change is occurring at the reaction center in going from proton abstraction by a very weak base (water) to stronger bases (buffers used in present study) to very strong bases (hydroxide ion) would be to study the effects of electron-withdrawing and electron-donating groups on both the pKa and ionization kinetics of 4′-substituted 2-phenyl-1,3-indandiones. Such a study will be reported separately (38).

In summary, the ionization kinetics of phenindione in aqueous solution appear to be qualitatively similar to those of phenylbutazone, but quantitative differences do occur. A study of the effect of various bases in promoting proton abstraction from phenindione has led to some insights into possible rate-determining transition states for the deprotonation reaction. The various rate constants calculated for proton donation and abstraction during phenindione ionization are substantially slower than the diffusion-limited constants for the ionization of normal or classical acids such as carboxylic, phenolic, and nitrogen acids. The ionization kinetics generated from this work will be used along with ongoing mass transport studies to predict the effect of noninstantaneous ionization kinetics on the mass transport behavior of carbon acids.

REFERENCES

(1) Y. Linaberg, O. Neiland, A. Veis, A. N. Latv, and G. Vanag, *Dokl. Akad. SSSR*, **154**, 1385 (1964); *Engl. Transl.*, **154**, 184 (1964).

(2) W. Sztark, *Diss. Pharm. Pharmacol.*, **19**, 429 (1968).

(3) J. G. Lombardino and E. H. Wiseman, *J. Med. Chem.*, **11**, 342 (1968).

(4) V. J. Stella and J. D. Pipkin, *J. Pharm. Sci.*, **65**, 1161 (1976).

(5) V. Stella, *ibid.*, **64**, 706 (1975).

(6) M. L. Bender, "Mechanisms of Homogeneous Catalysis from Protons to Proteins", Wiley–Interscience, New York, N.Y. 1971, chap. 2.

(7) M. Eigen, *Angew. Chem. Int. Ed.*, **3**, 1 (1964).

(8) J. R. Jones, *Prog. Phys. Org. Chem.*, **9**, 241 (1972).

(9) A. J. Kresge, *Acc. Chem. Res.*, **8**, 354 (1975).

(10) R. P. Bell and S. Grainger, *J. Chem. Soc. Perkin Trans. II*, **1976**, 1367.

(11) T. Riley and F. A. Long, *J. Am. Chem. Soc.*, **84**, 522 (1962).

(12) R. F. Pratt and T. C. Bruice, *J. Org. Chem.*, **37**, 3563 (1972).

(13) F. G. Bordwell and W. J. Boyle, Jr., *J. Am. Chem. Soc.*, **97**, 3447 (1975).

(14) *Ibid.*, **93**, 512 (1971).

(15) F. G. Bordwell, W. J. Boyle, Jr., J. A. Hautala, and K. C. Lee, *J. Am. Chem. Soc.*, **91**, 4002 (1969).

(16) F. G. Bordwell, W. J. Boyle, Jr., and K. C. Lee, *ibid.*, **92**, 5926 (1970).

(17) F. G. Bordwell and W. J. Boyle, Jr., *ibid.*, **93**, 511 (1971).

(18) *Ibid.*, **94**, 3907 (1972).

(19) D. J. Hupe and D. Wu, *J. Am. Chem. Soc.*, **99**, 7653 (1977).

(20) A. J. Kresge, D. A. Drake, and Y. Chang, *Can. J. Chem.*, **52**, 1889 (1974).

(21) J.-H. Kim and K. T. Leffek, *ibid.*, **52**, 592 (1974).

(22) D. J. Barnes and R. P. Bell, *Proc. R. Soc. London A*, **318**, 421 (1970).

(23) A. J. Kresge, *Chem. Soc. Rev.*, **2**, 475 (1973).

(24) R. P. Bell and R. G. Pearson, *J. Chem. Soc.*, **1953**, 3443.

(25) H. J. den Hertog and W. P. Combé, *Recueil*, **70**, 589 (1951).

(26) A. Albert and E. P. Serjeant, "Ionization Constants of Acids and Bases," Metheun, London, England, 1962.

(27) O. Kajimoto, T. Saeki, Y. Nagaoka, and T. Fueno, *J. Phys. Chem.*, **81**, 1712 (1977).

(28) J. L. Anderson, E. M. Eyring, and M. P. Whittaker, *ibid.*, **68**, 1128 (1964).

(29) R. K. Momu and N. H. Nachtrieb, *Inorg. Chem.*, **6**, 1189 (1967).

(30) N. Ingri, G. Lagerstrom, M. Frydman, and L. G. Sillén, *Acta Chem. Scand.*, **11**, 1034 (1957).

(31) N. Ingri, *ibid.*, **16**, 439 (1962).

(32) *Ibid.*, **17**, 573 (1963).

(33) *Ibid.*, **17**, 581 (1963).

(34) J. N. Brønsted and K. Pederson, *Z. Phys. Chem.*, **108**, 185 (1924).

(35) R. A. Marcus, *J. Phys. Chem.*, **72**, 891 (1968).
(36) G. C. Pimentel and A. L. McClellan, "The Hydrogen Bond," W. H. Freeman, San Francisco, Calif. 1960, chap. 6.
(37) G. S. Rork and I. H. Pitman, *J. Am. Chem. Soc.*, **96**, 4654 (1974).
(38) V. J. Stella and R. Gish, *J. Pharm. Sci.*, **68**, 1047 (1979).

ACKNOWLEDGMENTS

Supported by Grant GM 22357 from the National Institutes of Health.

The authors thank Dr. R. Schowen for valuable discussions and assistance.

Kinetics and Mechanism of Ionization of the Carbon Acids 4′-Substituted 2-Phenyl-1,3-indandiones

V. J. STELLA ˣ and R. GISH

Received December 14, 1978, from the *Department of Pharmaceutical Chemistry, University of Kansas, Lawrence, KS 66045.* Accepted for publication February 20, 1979.

Abstract □ The ionization kinetics of 1,3-diketone carbon acids are slow relative to those of classical acids and bases. The ionization kinetics of three 4′-substituted 2-phenyl-1,3-indandiones, 4′-chloro-, 4′-methoxy-, and 2-phenyl-1,3-indandione itself, were studied at 25° and ionic strength 0.1 using stopped-flow spectrometry and a pH jump technique. A log k'_{obs}–pH profile for the approach to the ionization equilibrium was consistent with a reaction scheme postulated earlier for the ionization of another carbon acid, phenylbutazone. The percent enol *versus* diketo form of the acids and the pKa_{enol} and pKa_{diketo} were calculated from the kinetic data. Hammett plots of the various kinetic and equilibrium constants supported a mechanism for acid deprotonation consistent with proton abstraction being the predominant process when very weak bases such as water were the proton acceptors. Desolvation effects and the work required to get the two reacting molecules together in the correct configurations predominated when the proton abstraction was by stronger proton acceptors.

Keyphrases □ Carbon acids—ionization kinetics, stopped-flow spectrophotometric and pH jump analysis □ Ionization kinetics—carbon acids, anisindione, phenindione, clorindione □ Anticoagulants—anisindione, phenindione, clorindione, ionization kinetics

The objective of this study was to compare the kinetics and ionization of the 1,3-diketone carbon acids anisindione (I), phenindione (II), and clorindione (III). All three compounds are used clinically as anticoagulants. The ionization kinetics of phenindione and phenylbutazone, two carbon acids of pharmaceutical interest, were reported previously (1, 2). Kinetic data for the deprotonation of various carbon acids have appeared in the chemical literature, but few studies of the effects of electron-withdrawing and electron-donating groups on the ionization kinetics and mechanism have been reported. The reported chemical studies have concerned acids of fairly high pKa (3, 4) or substituted nitromethane carbon acids (3, 5–12).

The objectives of this work were to study the effects of electron-withdrawing and electron-donating substituents

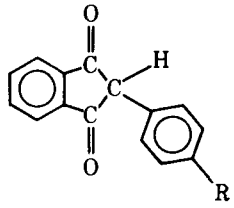

I: R = OCH_3
II: R = H
III: R = Cl

on ionization kinetics of I–III and to determine whether the results supported a model proposed previously for phenindione ionization (1).

EXPERIMENTAL

Phenindione[1] and anisindione[2] were used as received. Clorindione was prepared by the reaction of phthalide and *p*-chlorobenzaldehyde in a sodium ethoxide–ethanol solution using a literature procedure (13) for the synthesis of various 2-phenyl-1,3-indandiones. All other materials, kinetic procedures, conditions, and methods of pKa determination were identical to those described previously (1).

RESULTS AND DISCUSSION

The macroscopic dissociation constants for I–III, determined spectrophotometrically in aqueous solution at 25° and $\mu = 0.1$, are given in Table I. These values compare favorably with the literature values for the pKa's when solvent differences are considered.

Figure 1 is a plot of log k'_{obs} *versus* pH for the approach to ionization equilibrium for I–III. The rate constant k'_{obs} is the pseudo-first-order observed rate constant for the approach to ionization equilibrium extrapolated to zero buffer concentration. A possible model for the ionization kinetics of I–III is given in Scheme I. This model is identical to the scheme postulated previously for phenylbutazone ionization (2).

The predominant neutral form of I–III in aqueous solution is the diketo species, K, rather than the enol species, E (14). The dissociated form of I–III is the so-called mesomeric anion, E^- (17). The macroscopic dissociation constant K_a, the percent enol, and k'_{obs} for the approach to ionization equilibrium in the absence of buffers are best described by Eqs. 1–3 (2):

$$\frac{1}{K_a} = \frac{1}{K_{a,enol}} + \frac{1}{K_{a,diketo}} \quad \text{(Eq. 1)}$$

$$\% \text{ enol} = \frac{K_{a,diketo}}{K_{a,enol} + K_{a,diketo}}\left(\frac{100}{1}\right) \quad \text{(Eq. 2)}$$

$$k'_{obs} = k_1 + k_3[OH^-] + \frac{k_2[H^+]K_{a,enol}}{K_{a,enol} + [H^+]} + \frac{k_4 K_{a,enol}}{K_{a,enol} + [H^+]} \quad \text{(Eq. 3)}$$

Table I—Macroscopic Ionization Constants for Anisindione, Phenindione, and Clorindione Determined Spectrophotometrically at 25 ± 0.1° and $\mu = 0.1$ with Sodium Chloride

Compound, Wavelength Used, nm	pKa	Literature pKa Values
Anisindione, 330	4.13	4.09 (14), 4.25 (15), 5.6 (16)
Phenindione, 326	4.09	4.10 (14), 4.13 (15), 5.4 (16)
Clorindione, 284	3.59	3.54 (14), 3.72 (15), 4.8 (16)

[1] Pfaltz and Bauer, Flushing, N.Y.
[2] Schering Corp., Bloomfield, N.J.

0022-3549/79/0800-1047$01.00/0